THE EUROPEAN
PHYSICAL JOURNAL B

Jeans type instability for a chemotactic model of cellular aggregation

P.H. Chavanis[a]

Laboratoire de Physique Théorique, Université Paul Sabatier, 118 route de Narbonne 31062 Toulouse Cedex, France

Abstract. We consider an inertial model of chemotactic aggregation generalizing the Keller-Segel model and we study the linear dynamical stability of an infinite and homogeneous distribution of cells (bacteria, amoebae, endothelial cells, ...) when inertial effects are accounted for. These inertial terms model cells directional persistence. We determine the condition of instability and the growth rate of the perturbation as a function of the cell density and the wavelength of the perturbation. We discuss the differences between overdamped (Keller-Segel) and inertial models. Finally, we show the analogy between the instability criterion for biological populations and the Jeans instability criterion in astrophysics.

PACS. 05.45.-a Nonlinear dynamics and chaos – 87.10.+e General theory and mathematical aspects – 89.20.-a Interdisciplinary applications of physics

1 Introduction

The self-organization of biological cells (bacteria, amoebae, endothelial cells, ...) or even insects (like ants) due to the long-range attraction of a chemical (pheromone, smell, food, ...) produced by the organisms themselves is a long-standing problem in physical sciences [1]. This process is called chemotaxis. The chemotactic aggregation of biological populations is usually studied in terms of the Keller-Segel model [2]:

$$\xi \frac{\partial \rho}{\partial t} = \nabla \cdot (D_2 \nabla \rho - D_1 \nabla c), \tag{1}$$

$$\epsilon \frac{\partial c}{\partial t} = -k(c)c + \rho f(c) + D\Delta c, \tag{2}$$

which consists in a drift-diffusion equation (1) governing the evolution of the density of cells $\rho(\mathbf{r}, t)$ coupled to a diffusion equation (2) involving terms of source and degradation for the secreted chemical $c(\mathbf{r}, t)$. The chemical is produced by the organisms (cells) at a rate $f(c)$ and is degraded at a rate $k(c)$. It also diffuses according to Fick's law with a diffusion coefficient D. The concentration of cells changes as a result of an oriented chemotactic motion in a direction of a positive gradient of the chemical and a random motion analogous to diffusion. In equation (1), $D_2(\rho, c)$ is the diffusion coefficient of the cells and $D_1(\rho, c)$ is a measure of the strength of the influence of the chemical gradient on the flow of cells. These coefficients depend a priori on the concentration of cells and on the concentration of the chemical. The Keller-Segel model is able to

reproduce the chemotactic aggregation (collapse) of biological populations when the attractive drift term $D_1 \nabla c$ overcomes the diffusive term $D_2 \nabla \rho$.

However, recent experiments of in vitro formation of blood vessels show that cells randomly spread on a gel matrix autonomously organize to form a connected vascular network that is interpreted as the beginning of a vasculature [3]. This phenomenon is responsible of angiogenesis, a major actor for the growth of tumors. These networks cannot be explained by the *parabolic model* (1)-(2) that leads to pointwise blow-up. However, they can be recovered by *hyperbolic models* that lead to the formation of networks patterns that are in good agreement with experimental results. These models take into account inertial effects and they have the form of hydrodynamic equations [3]:

$$\frac{\partial \rho}{\partial t} + \nabla \cdot (\rho \mathbf{u}) = 0, \tag{3}$$

$$\frac{\partial \mathbf{u}}{\partial t} + (\mathbf{u} \cdot \nabla)\mathbf{u} = -\frac{1}{\rho} \nabla p + \nabla c, \tag{4}$$

$$\frac{\partial c}{\partial t} = -kc + f\rho + D_c \Delta c. \tag{5}$$

The inertial term models cells directional persistence and the general density dependent pressure term $-\nabla p(\rho)$ can take into account the fact that the cells do not interpenetrate. In these models, the particles concentrate on lines or filaments [3,4]. These structures share some analogies with the formation of ants' networks (due to the attraction of a pheromonal substance) and with the large-scale structures in the universe that are described by similar hydrodynamic (hyperbolic) equations, the Euler-Poisson

---
[a] e-mail: `chavanis@irsamc.ups-tlse.fr`

system [5]. The similarities between the networks observed in astrophysics (see Figs. 10, 11 of [6]) and biology (see Figs. 1, 2 of [3]) are striking. In order to make the connection between the parabolic model (1)-(2) and the hyperbolic model (3)-(5), we consider a model of the form

$$\frac{\partial \rho}{\partial t} + \nabla \cdot (\rho \mathbf{u}) = 0, \tag{6}$$

$$\rho \left[\frac{\partial \mathbf{u}}{\partial t} + (\mathbf{u} \cdot \nabla)\mathbf{u} \right] = -D_2 \nabla \rho + D_1 \nabla c - \xi \rho \mathbf{u}, \tag{7}$$

$$\epsilon \frac{\partial c}{\partial t} = -k(c)c + \rho f(c) + D\Delta c, \tag{8}$$

including a friction force $-\xi \rho \mathbf{u}$. This type of damped hydrodynamic equations was introduced in [7,8] at a general level. This inertial model takes into account the fact that the particles do not respond immediately to the chemotactic drift but that they have the tendency to continue in a given direction on their own. However, after a relaxation time of order ξ^{-1}, their velocity will be aligned with the chemotactic gradient. This is modeled by an effective friction force in equation (7) where the friction coefficient $\xi \sim \tau^{-1}$ is interpreted as the inverse of the relaxation time. This term can also represent a physical friction of the organisms against a fixed matrigel. In the strong friction limit $\xi \to +\infty$, or for large times $t \gg \xi^{-1}$, one can formally neglect the inertial term in equation (7) and obtain [8–10]:

$$\rho \mathbf{u} = -\frac{1}{\xi} (D_2 \nabla \rho - D_1 \nabla c) + O(\xi^{-2}). \tag{9}$$

Substituting this relation in equation (6), we recover the parabolic Keller-Segel model (1)-(2). Therefore, the Keller-Segel model can be viewed as an overdamped limit of a hydrodynamic model involving a friction force. Alternatively, neglecting the friction force $\xi = 0$, we recover the hydrodynamic model introduced in [3].

In this paper, we study the linear dynamical stability of an infinite and homogeneous distribution of cells with respect to the inertial model (6)-(8). We determine the condition of instability and the growth rate of the perturbation, and discuss the differences with the results obtained with the Keller-Segel model (1)-(2). We also discuss some analogies with the dynamical stability of self-gravitating systems. Indeed, there are many analogies between the chemotactic aggregation of biological populations and the dynamics of self-gravitating Brownian particles [9]. In particular, the Keller-Segel model (1)–(2) is similar to the Smoluchowski-Poisson system [11] and the hydrodynamic equations (6)-(8) are similar to the damped Euler equations of Brownian particles [8,10]. The main difference between biological systems and self-gravitating Brownian particles is that the Poisson equation in the gravitational problem is replaced by a more general field equation (8) taking into account the specificities of the biological problem. Owing to this analogy, we shall discuss the relation between the instability criterion of biological populations and the Jeans instability criterion [12] in astrophysics.

2 Instability criterion for biological populations

2.1 The dispersion relation

We consider an infinite and homogeneous stationary solution of equations (6–8) with $\mathbf{u} = \mathbf{0}$, $\rho = $ Cst. and $c = $ Cst. such that

$$k(c)c = f(c)\rho. \tag{10}$$

Linearizing the equations around this stationary solution, we get

$$\frac{\partial \delta \rho}{\partial t} + \rho \nabla \cdot \delta \mathbf{u} = 0, \tag{11}$$

$$\rho \frac{\partial \delta \mathbf{u}}{\partial t} = -D_2 \nabla \delta \rho + D_1 \nabla \delta c - \xi \rho \delta \mathbf{u}, \tag{12}$$

$$\epsilon \frac{\partial \delta c}{\partial t} = (f'(c)\rho - \overline{k})\delta c + f(c)\delta \rho + D\Delta \delta c, \tag{13}$$

where we have set $\overline{k} = k(c) + ck'(c)$. Eliminating the velocity between equations (11) and (12), we obtain

$$\frac{\partial^2 \delta \rho}{\partial t^2} + \xi \frac{\partial \delta \rho}{\partial t} = D_2 \Delta \delta \rho - D_1 \Delta \delta c. \tag{14}$$

Looking for solutions of the form $\delta \rho \sim \delta \hat{\rho} e^{\sigma t} e^{i\mathbf{q} \cdot \mathbf{r}}$ and $\delta c \sim \delta \hat{c} e^{\sigma t} e^{i\mathbf{q} \cdot \mathbf{r}}$, we get

$$(F - \epsilon \sigma)\delta \hat{c} + f(c)\delta \hat{\rho} = 0, \tag{15}$$

$$D_1 q^2 \delta \hat{c} - (D_2 q^2 + \sigma(\sigma + \xi))\delta \hat{\rho} = 0, \tag{16}$$

where $F = f'(c)\rho - \overline{k} - q^2 D$. These equations have nontrivial solutions only if the determinant of the system is equal to zero yielding the dispersion relation

$$\epsilon \sigma^3 + (\epsilon \xi - F)\sigma^2 - (F\xi - \epsilon q^2 D_2)\sigma$$
$$- q^2(f(c)D_1 + D_2 F) = 0. \tag{17}$$

The condition of marginal stability ($\sigma = 0$) corresponds to $f(c)D_1 + D_2 F = 0$ and the condition of instability is

$$f(c)D_1 + D_2 F > 0. \tag{18}$$

We note that the instability criterion does not depend on the value of ϵ and ξ. Let us consider in detail some particular cases.

2.2 The case $\epsilon = 0$

When the chemical has a large diffusivity, the temporal term in equation (8) can be neglected [13]. Thus, we formally consider $\epsilon = 0$. In that case, the dispersion relation (17) reduces to

$$\sigma^2 + \xi \sigma + q^2 \left(D_2 + \frac{f(c)D_1}{F} \right) = 0. \tag{19}$$

The discriminant is

$$\Delta(q) = \xi^2 - 4q^2 \left(D_2 + \frac{f(c)D_1}{F(q)} \right), \qquad (20)$$

and the two roots are

$$\sigma_\pm = \frac{-\xi \pm \sqrt{\Delta(q)}}{2}. \qquad (21)$$

If $R_e(\sigma) < 0$ the perturbation decays exponentially rapidly and if $R_e(\sigma) > 0$ the perturbation grows exponentially rapidly. In that case, the system is unstable and $R_e(\sigma)$ is the growth rate of the perturbation. If $D_2 + f(c)D_1/F < 0$, then $\Delta > \xi^2$ so that $\sigma_+ > 0$ (unstable). Alternatively, if $D_2 + f(c)D_1/F \geq 0$, then $\Delta \leq \xi^2$. Either $\Delta \leq 0$ and $R_e(\sigma) = -\xi/2 \leq 0$ (stable) or $0 \leq \Delta \leq \xi^2$ and $\sigma_\pm \leq 0$ (stable). Therefore, the system is unstable if

$$D_2 < \frac{f(c)D_1}{\overline{k} - f'(c)\rho + Dq^2}, \qquad (22)$$

and stable otherwise. To determine the range of unstable wavelengths, we must consider different cases:

2.2.1 If $\overline{k} - f'(c)\rho \geq 0$

In that case, a *necessary* condition of instability is that

$$D_2 < \frac{f(c)D_1}{\overline{k} - f'(c)\rho} \equiv (D_2)_{crit}. \qquad (23)$$

If this condition is fulfilled, the unstable wavenumbers are determined by

$$q^2 \leq \frac{1}{D} \left[\frac{f(c)D_1}{D_2} + f'(c)\rho - \overline{k} \right] \equiv q_{max}^2. \qquad (24)$$

The growth rate of the perturbation with wavenumber q is $\sigma_+ = \frac{1}{2}(-\xi + \sqrt{\Delta(q)})$. Therefore, the most unstable mode q_* is the one which maximizes $\Delta(q)$. It is given by

$$Dq_*^2 = \left[\frac{f(c)D_1(\overline{k} - f'(c)\rho)}{D_2} \right]^{1/2} + f'(c)\rho - \overline{k}. \qquad (25)$$

The largest growth rate σ_* is then determined by

$$2\sigma_* = -\xi + \sqrt{\xi^2 + \frac{4f(c)D_1}{D} \left(1 - \sqrt{\frac{D_2(\overline{k} - f'(c)\rho)}{f(c)D_1}} \right)^2}. \qquad (26)$$

In particular, for $\xi = 0$, we have

$$2\sigma_* = \sqrt{\frac{4f(c)D_1}{D}} \left(1 - \sqrt{\frac{D_2(\overline{k} - f'(c)\rho)}{f(c)D_1}} \right). \qquad (27)$$

The range of unstable wavelengths is determined graphically in Figure 1 and the evolution of the growth rate of the perturbation as a function of the wavenumber is plotted in Figure 2 (we have also consider the case $\epsilon \neq 0$ in this figure by solving equation (17) which is a second degree equation in $x = q^2$).
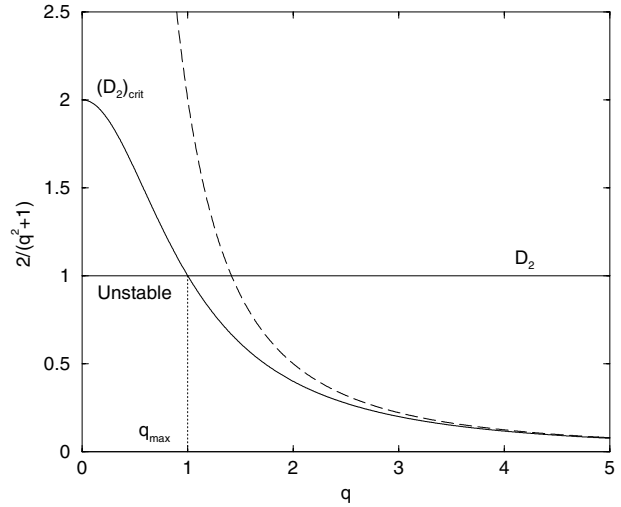

Fig. 1. Graphical construction determining the range of unstable wavenumbers. We have taken $\xi = D_2 = D = 1$, $fD_1 = 2$ and $\overline{k} - f'(c)\rho = 1$ (solid line) or $\overline{k} - f'(c)\rho = 0$ (dashed line).
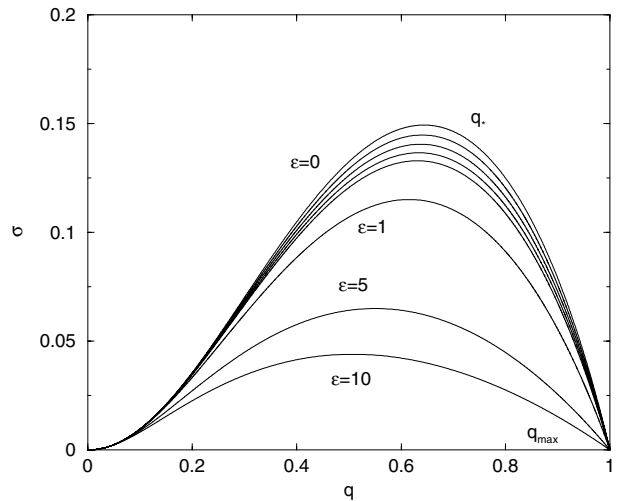

Fig. 2. Evolution of the growth rate of the perturbation as a function of the wavenumber for different values of ϵ. We have taken $\xi = D_2 = D = 1$, $fD_1 = 2$ and $\overline{k} - f'(c)\rho = 1$.

2.2.2 If $\overline{k} - f'(c)\rho = 0$

In that case, $(D_2)_{crit} = +\infty$. The unstable wavenumbers are determined by

$$q^2 \leq \frac{f(c)D_1}{DD_2} \equiv q_{max}^2. \qquad (28)$$

The most unstable mode is $q_* = 0$ and the largest growth rate σ_* is given by

$$2\sigma_* = -\xi + \sqrt{\xi^2 + \frac{4f(c)D_1}{D}}. \qquad (29)$$

2.2.3 If $\overline{k} - f'(c)\rho < 0$

In that case, the system is unstable for

$$\frac{f'(c)\rho - \overline{k}}{D} \leq q^2 \leq \frac{1}{D}\left[\frac{f(c)D_1}{D_2} + f'(c)\rho - \overline{k}\right]. \quad (30)$$

The growth rate diverges when

$$q^2 \to \frac{f'(c)\rho - \overline{k}}{D} \equiv q_0^2, \quad (31)$$

corresponding to $F(q) = 0$. Close to the critical wavenumber q_0, we have

$$\sigma \sim \left(\frac{q_0 f(c)D_1}{2D}\right)^{1/2}\frac{1}{\sqrt{q - q_0}}, \quad (q \to q_0^+). \quad (32)$$

This expression is valid for ξ finite and $\epsilon = 0$. It can be directly obtain from equation (19) by using $F \sim -2Dq_0(q - q_0) \to 0$ for $q \to q_0$. Thus, when the temporal term is neglected in equation (8), i.e. $\epsilon = 0$, a critical behaviour occurs. This critical behaviour is regularized for $\epsilon \neq 0$. Indeed, taking $q = q_0$, i.e. $F = 0$, in equation (17), we obtain

$$\epsilon\sigma^3 + \epsilon\xi\sigma^2 + \epsilon q_0^2 D_2\sigma - q_0^2 f(c)D_1 = 0. \quad (33)$$

Taking the limit $\epsilon \to 0$, we find that

$$\sigma(q_0) \sim \left(\frac{q_0^2 f(c)D_1}{\epsilon}\right)^{1/3}, \quad (34)$$

which is finite for $\epsilon > 0$ but diverges like $\epsilon^{-1/3}$ when $\epsilon \to 0$. For $\epsilon \to 0$ and $q \to q_0$, the dispersion relation can be simplified in

$$\epsilon\sigma^3 + 2Dq_0(q - q_0)\sigma^2 - q_0^2 f(c)D_1 = 0. \quad (35)$$

For $\epsilon = 0$ we recover equation (32) and for $q = q_0$ we recover equation (34). For $q \to q_0$, we can easily express q as a function of σ according to

$$q - q_0 = \frac{q_0^2 f(c)D_1 - \epsilon\sigma^3}{2Dq_0\sigma^2}. \quad (36)$$

On the other hand, for $q = 0$, equation (17) reduces to

$$\epsilon\sigma^3 + (\xi\epsilon - f'(c)\rho + \overline{k})\sigma^2 - \xi(f'(c)\rho - \overline{k})\sigma = 0. \quad (37)$$

The positive root of this equation is

$$\sigma(0) = \frac{f'(c)\rho - \overline{k}}{\epsilon} = \frac{Dq_0^2}{\epsilon}, \quad (38)$$

which is finite for $\epsilon > 0$ but diverges like ϵ^{-1} when $\epsilon \to 0$.

The range of unstable wavenumbers is determined graphically in Figure 3 and the evolution of the growth rate of the perturbation as a function of the wavenumber is plotted in Figure 4 (we have also consider the case $\epsilon \neq 0$ in this figure by solving Eq. (17)). We see that the case
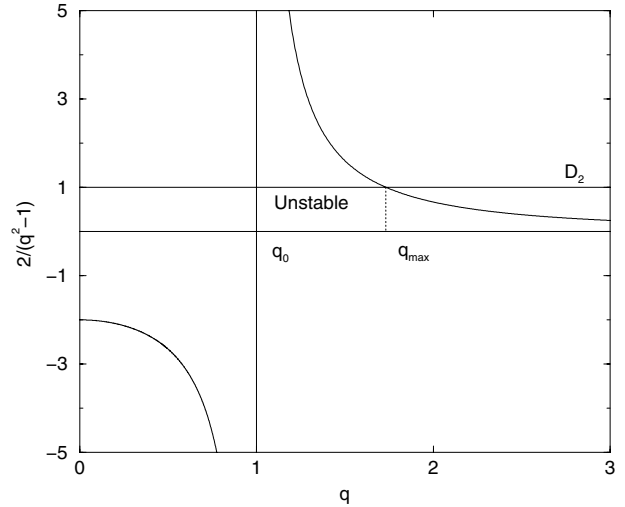

Fig. 3. Graphical construction determining the range of unstable wavenumbers. We have taken $\xi = D_2 = D = 1$, $fD_1 = 2$ and $\overline{k} - f'(c)\rho = -1$.
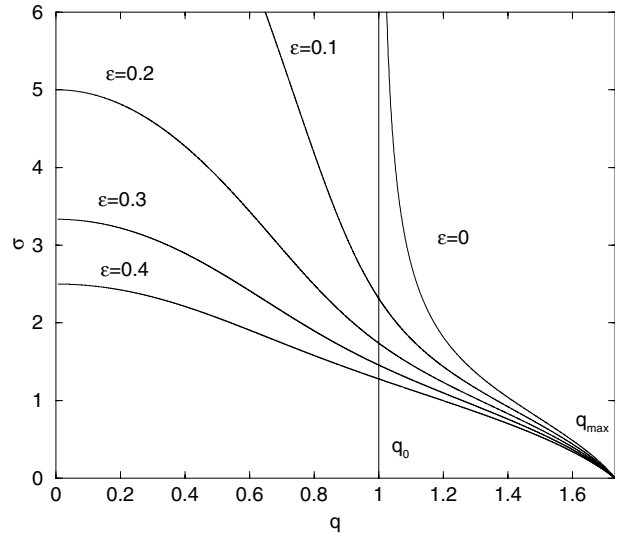

Fig. 4. Evolution of the growth rate of the perturbation as a function of the wavenumber. We have taken $\xi = D_2 = D = 1$, $fD_1 = 2$ and $\overline{k} - f'(c)\rho = -1$.

$\epsilon = 0$ is very special. For $\epsilon = 0$, the range of wavenumbers $q < q_0$ seems to be stable according to equation (30) because the two roots of equation (19) are negative. However, for any finite value of ϵ, a third root appears. This root is positive and tends to infinity when $\epsilon \to 0$ (see Eqs. (34) and (38)). Therefore, this unstable branch is rejected to infinity when $\epsilon \to 0$. This implies that the region $q < q_0$ is in fact extremely unstable for $\epsilon = 0^+$. In particular, for $\epsilon > 0$, the most unstable mode is $q_* = 0$ and the largest growth rate is given by equation (38).

2.3 The case $\xi \to +\infty$

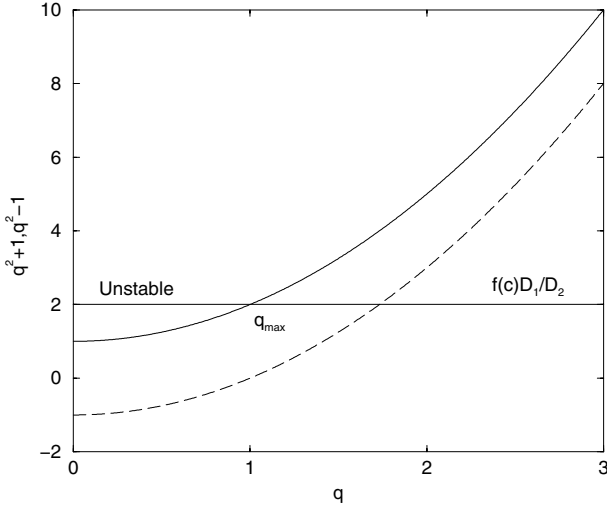In the overdamped limit, the hydrodynamical equations (6–8) return the Keller-Segel model (1)-(2). Let us

Fig. 5. Graphical construction determining the range of unstable wavenumbers. We have taken $D_2 = D = 1$, $fD_1 = 2$ and $\overline{k} - f'(c)\rho = 1$ (solid line) and $\overline{k} - f'(c)\rho = -1$ (dashed line).

consider the stability analysis in that case for comparison with the inertial case. The dispersion relation now reads

$$\epsilon\xi\sigma^2 - (F\xi - \epsilon q^2 D_2)\sigma - q^2(f(c)D_1 + D_2 F) = 0, \quad (39)$$

and the two roots are

$$\sigma_{\pm} = \frac{F\xi - \epsilon D_2 q^2 \pm \sqrt{\Delta(q)}}{2\epsilon\xi}, \quad (40)$$

where

$$\Delta(q) = (F\xi + \epsilon q^2 D_2)^2 + 4\epsilon\xi q^2 f(c)D_1 \geq 0. \quad (41)$$

Writing the solution in the form

$$\sigma = \frac{-b \pm \sqrt{b^2 - 4ac}}{2a}, \quad (42)$$

it is easy to see that the system is stable if (i) $F < \epsilon q^2 D_2/\xi$ ($b > 0$) and if (ii) $F < -f(c)D_1/D_2$ ($c > 0$). It is unstable otherwise. Since (ii) implies (i), the system is stable if $F < -f(c)D_1/D_2$ and unstable otherwise. Thus, the system is unstable if

$$\overline{k} - f'(c)\rho + Dq^2 < \frac{f(c)D_1}{D_2}, \quad (43)$$

and stable otherwise. The range of unstable wavenumbers is determined graphically in Figure 5.

2.3.1 If $\overline{k} - f'(c)\rho \geq 0$

In that case, the system is unstable for

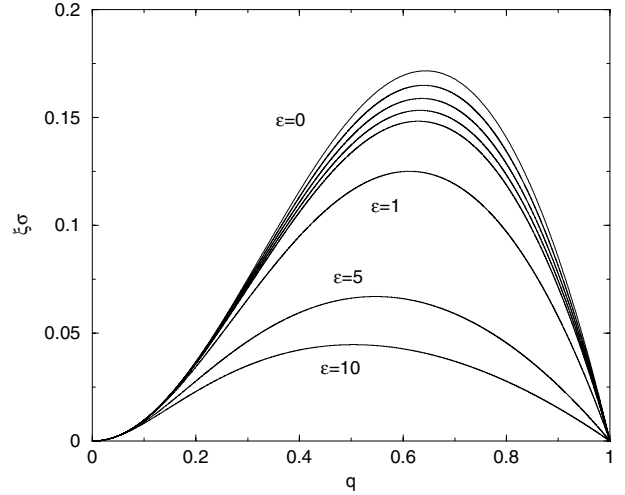$$D_2 < \frac{f(c)D_1}{\overline{k} - f'(c)\rho + Dq^2}, \quad (44)$$

Fig. 6. Evolution of the growth rate of the perturbation as a function of the wavenumber for the Keller-Segel model. We have taken $D_2 = D = 1$, $fD_1 = 2$ and $\overline{k} - f'(c)\rho = 1$.

and stable otherwise. This is the same criterion as for the inertial model. A *necessary* condition of instability is that

$$D_2 < \frac{f(c)D_1}{\overline{k} - f'(c)\rho} \equiv (D_2)_{crit}. \quad (45)$$

If this condition is fulfilled, the unstable wavenumbers are such that

$$q^2 \leq \frac{1}{D}\left[\frac{f(c)D_1}{D_2} + f'(c)\rho - \overline{k}\right] \equiv q_{max}^2. \quad (46)$$

These results are unchanged with respect to the inertial case.

We now determine the value of the optimal (most unstable) wavenumber q_* and the corresponding growth rate σ_* (see Fig. 6). Equation (39) is a second order equation in σ whose solutions are given by equation (40). We can maximize $\sigma_+(q)$ to obtain q_* and σ_*. However, it appears simpler to proceed differently. Equation (39) can also be viewed as a second order equation in $x = q^2$ of the form

$$Ax^2 + B(\sigma)x + C(\sigma) = 0, \quad (47)$$

with

$$A = DD_2, \quad (48)$$
$$B(\sigma) = (D\xi + \epsilon D_2)\sigma - f(c)D_1 - D_2(f'(c)\rho - \overline{k}), \quad (49)$$
$$C(\sigma) = \epsilon\xi\sigma^2 - \xi(f'(c)\rho - \overline{k})\sigma \geq 0. \quad (50)$$

There will be two roots x_1 and x_2 provided that $B(\sigma) < 0$ and $\Delta(\sigma) = B^2 - 4AC \geq 0$. This last condition can be written

$$\Delta(\sigma) \equiv a\sigma^2 + b\sigma + c \geq 0, \quad (51)$$

with

$$a = (D\xi - \epsilon D_2)^2, \tag{52}$$

$$b = -2[D_2(f(c)D_1 + D_2(f'(c)\rho - \overline{k}))\epsilon$$
$$\quad + D\xi f(c)D_1 - DD_2\xi(f'(c)\rho - \overline{k})] < 0, \tag{53}$$

$$c = [f(c)D_1 + D_2(f'(c)\rho - \overline{k})]^2. \tag{54}$$

The discriminant $\delta = b^2 - 4ac$ of equation (51) is given by

$$\delta = 16f(c)\xi DD_1 D_2[(f(c)D_1$$
$$+D_2(f'(c)\rho - \overline{k}))\epsilon - D\xi(f'(c)\rho - \overline{k})]. \tag{55}$$

The condition $\Delta(\sigma) \geq 0$ to have two roots x_1 and x_2 is equivalent to $\sigma \leq \sigma_*$ with

$$\sigma_* = \frac{-b - \sqrt{\delta}}{2a}. \tag{56}$$

(Note that the possibility $\sigma \geq (-b + \sqrt{\delta})/2a$ must be rejected since it does not satisfy the requirement $B(\sigma) < 0$). For $\sigma = \sigma_*$, the two roots $x_1 = x_2 = x_*$ coincide ($\Delta = 0$) so that σ_* is the maximum growth rate. It is reached for an optimal wavenumber $x_* = -B/(2A)$, i.e.

$$q_*^2 = \frac{-B(\sigma_*)}{2A}. \tag{57}$$

2.3.2 If $\overline{k} - f'(c)\rho < 0$

In that case the system is unstable for the wavenumbers

$$q^2 \leq \frac{1}{D}\left[\frac{f(c)D_1}{D_2} + f'(c)\rho - \overline{k}\right] \equiv q_{max}^2. \tag{58}$$

The growth rate of the perturbation as a function of the wavenumber is plotted in Figure 7. As discussed in Section 2.2.3, the case $\epsilon = 0$ is special and will be considered specifically in the next section.

2.4 The case $\xi \to +\infty$ and $\epsilon = 0$

If we neglect the temporal term ($\epsilon = 0$) in the Keller-Segel model ($\xi \to +\infty$), we obtain the dispersion relation

$$F\xi\sigma + q^2(f(c)D_1 + D_2F) = 0, \tag{59}$$

so that σ is explicitly given by

$$\xi\sigma = q^2\left(\frac{f(c)D_1}{Dq^2 + \overline{k} - f'(c)\rho} - D_2\right). \tag{60}$$

The instability criterion is given by equation (22).

2.4.1 If $\overline{k} - f'(c)\rho \geq 0$

This is a particular case of Section 2.2.1 corresponding to $\xi \to +\infty$. The expression of the largest growth rate is given by

$$\sigma_* = \frac{f(c)D_1}{\xi D}\left(1 - \sqrt{\frac{D_2(\overline{k} - f'(c)\rho)}{f(c)D_1}}\right)^2. \tag{61}$$
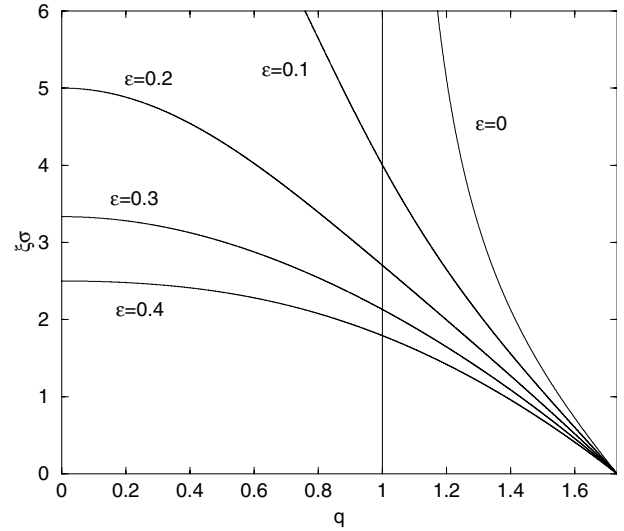
The other results are unchanged.

Fig. 7. Evolution of the growth rate of the perturbation as a function of the wavenumber for the Keller-Segel model. We have taken $D_2 = D = 1$, $fD_1 = 2$ and $\overline{k} - f'(c)\rho = -1$.

2.4.2 If $\overline{k} - f'(c)\rho < 0$

The system is unstable for the wavenumbers determined by equation (30). For $q \to q_0^+$, corresponding to $F \sim -2Dq_0(q - q_0) \to 0$, the growth rate diverges like

$$\xi\sigma \sim \frac{q_0 f(c)D_1}{2D(q - q_0)}. \tag{62}$$

This divergence is regularized if $\epsilon \neq 0$. Taking $q = q_0$, i.e. $F = 0$ in equation (39), we get

$$\epsilon\xi\sigma^2 + \epsilon q_0^2 D_2\sigma - q_0^2 f(c)D_1 = 0. \tag{63}$$

For $\epsilon \to 0$, we obtain

$$\sigma(q_0) \sim \left(\frac{q_0^2 f(c)D_1}{\xi\epsilon}\right)^{1/2}, \tag{64}$$

which is finite for $\epsilon > 0$ but diverges like $\epsilon^{-1/2}$ when $\epsilon \to 0$. For $\epsilon \to 0$ and $q \to q_0^+$, equation (39) can be simplified in

$$\epsilon\xi\sigma^2 + 2Dq_0\xi(q - q_0)\sigma - q_0^2 f(c)D_1 = 0. \tag{65}$$

For $\epsilon = 0$ we recover equation (62) and for $q = q_0$ we recover equation (64). The solution of equation (65) is

$$\epsilon\sigma = -Dq_0(q - q_0) + \sqrt{D^2 q_0^2(q - q_0)^2 + \frac{\epsilon q_0^2 f(c)D_1}{\xi}}. \tag{66}$$

On the other hand, for $q = 0$, equation (39) leads to

$$\sigma(0) = \frac{f'(c)\rho - \overline{k}}{\epsilon}, \tag{67}$$

which is finite for $\epsilon > 0$ but diverges like ϵ^{-1} when $\epsilon \to 0$.

Equations (32–34) and (62–64) differ because both σ and ξ tend to infinity, so that the expression depend on how the limits are taken. The general case can be treated as follows. For $\epsilon = 0$, taking $q \to q_0^+$ in equation (19) we get

$$\sigma(\sigma + \xi) \sim \frac{q_0 f(c) D_1}{2D(q - q_0)}. \tag{68}$$

On the other hand, for $\epsilon \neq 0$, taking $q = q_0$ (i.e. $F = 0$) in equation (17), we get

$$\sigma^2(\sigma + \xi) \sim \frac{q_0 f(c) D_1}{\epsilon}. \tag{69}$$

Finally, for $\epsilon \to 0$ and $q \to q_0$, we have

$$\epsilon \sigma^3 + (\epsilon \xi + 2D q_0(q - q_0))\sigma^2$$
$$+ 2D q_0(q - q_0)\xi\sigma - q_0^2 f(c) D_1 = 0. \tag{70}$$

which reproduces the correct behaviours (68) and (69).

3 Analogy with the Jeans problem in astrophysics

3.1 The damped Euler equations

Let us consider a particular case of equations (6–8) corresponding to $D_2(\rho, c) = p'(\rho)$ and $D_1(\rho, c) = \rho S'(c)$ where p and S are arbitrary functions. In that case, the hydrodynamical equations take the form

$$\frac{\partial \rho}{\partial t} + \nabla \cdot (\rho \mathbf{u}) = 0, \tag{71}$$

$$\frac{\partial \mathbf{u}}{\partial t} + (\mathbf{u} \cdot \nabla)\mathbf{u} = -\frac{1}{\rho}\nabla p + \nabla S(c) - \xi\mathbf{u}, \tag{72}$$

$$\epsilon \frac{\partial c}{\partial t} = -k(c)c + \rho f(c) + D\Delta c. \tag{73}$$

For $\xi \to +\infty$, we can neglect the inertia of the particles so that $\rho\mathbf{u} \simeq -\frac{1}{\xi}(\nabla p - \rho\nabla S(c))$. Substituting this relation in equation (71), we obtain a special case of the Keller-Segel model

$$\frac{\partial \rho}{\partial t} = \nabla \cdot [\chi(\nabla p - \rho S'(c)\nabla c)], \tag{74}$$

where we have set $\chi = 1/\xi$. Equations (71, 72) can be viewed as fluid equations appropriate to the chemotactic problem. Equation (71) is an equation of continuity and equation (72) is similar to the Euler equation where p plays the role of a pressure and the chemotactic attraction plays the role of a force. Since $p = p(\rho)$, these equations describe a barotropic fluid. The main novelty of these equations with respect to usual hydrodynamical equations is the presence of a friction force which allows to make a connection between hyperbolic ($\xi = 0$) and parabolic ($\xi \to +\infty$) models.

This hydrodynamic model including a friction force is similar to the damped barotropic Euler-Poisson system which describes a gas of self-gravitating Brownian particles [8,10] or the violent relaxation of collisionless stellar systems on the coarse-grained scale in astrophysics [7]. In that analogy, the concentration of the chemical c plays the role of the gravitational potential Φ. The main difference between the two models is that the Poisson equation for self-gravitating systems is replaced by a more general field equation (73) for bacterial populations. To emphasize the connection with astrophysical problems, let us consider a particular case of equations (71–73) where $\epsilon = 0$, $S(c) = c$ and k and f are constant. Then, introducing notations similar to those used in astrophysics (noting $c = -\Phi$, $k/D = k_0^2$, $f/D = S_d G$), we can rewrite equations (71–73) in the form

$$\frac{\partial \rho}{\partial t} + \nabla \cdot (\rho \mathbf{u}) = 0, \tag{75}$$

$$\frac{\partial \mathbf{u}}{\partial t} + (\mathbf{u} \cdot \nabla)\mathbf{u} = -\frac{1}{\rho}\nabla p - \nabla\Phi - \xi\mathbf{u}, \tag{76}$$

$$\Delta\Phi - k_0^2\Phi = S_d G(\rho - \overline{\rho}). \tag{77}$$

When $k_0 = \overline{\rho} = 0$, these equations are isomorphic to the damped Euler-Poisson system describing self-gravitating Brownian particles [8,10]. In the strong friction limit, we get

$$\frac{\partial \rho}{\partial t} = \nabla \cdot \left[\frac{1}{\xi}(\nabla p + \rho\nabla\Phi)\right], \tag{78}$$

which can be interpreted as a generalized Smoluchowski equation. Thus, for $\xi \to +\infty$, we obtain the generalized Smoluchowski-Poisson system describing self-gravitating Brownian particles in an overdamped limit [8]. Alternatively, for $\xi = 0$ we recover the barotropic Euler-Poisson system that has been studied at length in astrophysics to determine the period of stellar pulsations [14] and the formation of large-scale structures in cosmology [5]. Therefore, the chemotactic model (75)-(77) is similar to astrophysical models with additional terms. In the astrophysical context, the case $k_0 \neq 0$ would correspond to a shielding of the gravitational interaction on a typical length k_0^{-1}. This Yukawa shielding appears in theories where the graviton has a mass but in that case k_0 is very small which does not need to be the case in the biological problem.

We now consider the linear dynamical stability of an infinite and homogeneous solution of equations (75–77). By mapping equations (75–77) onto a generalized astrophysical model, we shall see that the instability criteria obtained in Section 2 are connected to (and extend) the Jeans instability criterion of astrophysics [12]. To avoid the Jeans swindle [15] when $k_0 = 0$, we have introduced a "neutralizing background" $\overline{\rho}$ in equation (77). In fact, in the biological problem, this term appears *naturally* when we consider the limit of large diffusivity of the chemical (see [13]); therefore, there is no "Jeans swindle" in the biological problem based on equation (2). A similar term $\overline{\rho}$ appears in cosmology when we take into account the expansion of the universe and work in the comoving frame [5].

3.2 The dispersion relation

We consider an infinite and homogeneous stationary solution of equations (75–77) with $\mathbf{u} = \mathbf{0}$, $\rho = $ Cst. and $\Phi = $ Cst. such that

$$-k_0^2\Phi = S_dG(\rho - \overline{\rho}).$$ (79)

For a pure Newtonian interaction with $k_0 = 0$, we have $\rho = \overline{\rho}$. Linearizing the equations around this stationary solution, we get

$$\frac{\partial \delta\rho}{\partial t} + \rho\nabla\cdot\delta\mathbf{u} = 0,$$ (80)

$$\rho\frac{\partial \delta\mathbf{u}}{\partial t} = -c_s^2\nabla\delta\rho - \rho\nabla\delta\Phi - \xi\rho\delta\mathbf{u},$$ (81)

$$\Delta\delta\Phi - k_0^2\delta\Phi = S_dG\delta\rho,$$ (82)

where we have introduced the velocity of sound $c_s^2 = p'(\rho)$. Eliminating the velocity between equations (80) and (81), we obtain

$$\frac{\partial^2\delta\rho}{\partial t^2} + \xi\frac{\partial\delta\rho}{\partial t} = c_s^2\Delta\delta\rho + \rho\Delta\delta\Phi.$$ (83)

Looking for solutions of the form $\delta\rho \sim \delta\hat\rho e^{i(\mathbf{k}\cdot\mathbf{r}-\omega t)}$, we get

$$(-\omega^2 - i\xi\omega + c_s^2k^2)\delta\hat\rho = -\rho k^2\delta\hat\Phi,$$ (84)

$$\delta\hat\Phi = -\frac{S_dG}{k^2 + k_0^2 - i\omega}\delta\hat\rho.$$ (85)

From these equations, we obtain the dispersion relation

$$\omega(\omega + i\xi) = c_s^2k^2 - \frac{S_dG\rho k^2}{k^2 + k_0^2}.$$ (86)

In the case $\xi = 0$ and $k_0 = 0$, we recover the usual Jeans dispersion relation [12]:

$$\omega^2 = c_s^2k^2 - S_dG\rho.$$ (87)

3.3 Instability criterion

If we set $\sigma = -i\omega$, the dispersion relation becomes

$$\sigma^2 + \xi\sigma + k^2\left(c_s^2 - \frac{S_dG\rho}{k^2 + k_0^2}\right) = 0.$$ (88)

The two roots are

$$\sigma = \frac{-\xi \pm \sqrt{\Delta(k)}}{2},$$ (89)

with

$$\Delta(k) = \xi^2 - 4k^2\left(c_s^2 - \frac{S_dG\rho}{k^2 + k_0^2}\right).$$ (90)

Accordingly, the system is unstable if

$$c_s^2 < \frac{S_dG\rho}{k^2 + k_0^2},$$ (91)

and stable otherwise. A necessary condition of instability is

$$c_s^2 < \frac{S_dG\rho}{k_0^2} \equiv (c_s^2)_{crit}.$$ (92)

If this condition is fulfilled the unstable wavelengths are such that

$$k \le \sqrt{\frac{S_dG\rho}{c_s^2} - k_0^2} \equiv k_{max}.$$ (93)

The wavelength which has the largest growth rate is given by

$$k_*^2 = \left(\frac{S_dG\rho k_0^2}{c_s^2}\right)^{1/2} - k_0^2,$$ (94)

and the corresponding growth rate is given by

$$2\sigma_* = -\xi + \sqrt{\xi^2 + 4S_dG\rho\left(1 - \sqrt{\frac{c_s^2k_0^2}{S_dG\rho}}\right)^2}.$$ (95)

The instability criterion (91) is equivalent to the instability criterion (22) of Section 2.2 for the particular case of the chemotactic model considered in Section 3.1. The parallel with astrophysics is interesting to develop in order to give a more physical interpretation to equation (22). All the other formulae can be interpreted accordingly. In particular, we note that the coefficient D_2 plays the role of a velocity of sound c_s^2.

3.4 Particular cases

Let us consider particular cases of the foregoing expressions:

• For $c_s = 0$, one has $k_{max} = +\infty$, $k_* = +\infty$ and

$$\sigma_* = \frac{-\xi + \sqrt{\xi^2 + 4S_dG\rho}}{2}.$$ (96)

• For $k_0 = 0$ (Newtonian potential), one has $(c_s^2)_{crit} = +\infty$, $k_{max} = (S_dG\rho/c_s^2)^{1/2} \equiv k_J$ (Jeans length), $k_* = 0$ and

$$\sigma_* = \frac{-\xi + \sqrt{\xi^2 + 4S_dG\rho}}{2}.$$ (97)

• For $\xi = 0$, one has

$$\sigma_* = (S_dG\rho)^{1/2}\left(1 - \sqrt{\frac{c_s^2k_0^2}{S_dG\rho}}\right).$$ (98)

• For $\xi \to +\infty$, one has

$$\sigma_* = \frac{S_dG\rho}{\xi}\left(1 - \sqrt{\frac{c_s^2k_0^2}{S_dG\rho}}\right)^2.$$ (99)

3.5 Isothermal gas

For an isothermal gas with an equation of state $p = \rho T$ (for simplicity, we have noted T instead of $k_B T/m$), the velocity of sound is equal to the square root of the temperature: $c_s^2 = T$. It is relevant to re-express the previous relations as follows. Introducing the critical temperature

$$T_c = \frac{S_d G \rho}{k_0^2}, \tag{100}$$

the growth rate of the perturbation can be written

$$\frac{2\sigma}{\xi} = -1 + \sqrt{1 - \frac{4 S_d G \rho}{\xi^2} \frac{k^2}{k_0^2} \left(\frac{T}{T_c} - \frac{1}{1 + (k/k_0)^2} \right)}. \tag{101}$$

The condition of instability reads

$$\frac{T}{T_c} \leq \frac{1}{1 + (k/k_0)^2}, \tag{102}$$

and a necessary condition of instability is $T < T_c$. For $T < T_c$ the unstable wavenumbers (see Fig. 8) are such that $k \leq k_{max}(T)$ with

$$\frac{k_{max}(T)}{k_0} = \sqrt{\frac{T_c}{T} - 1}. \tag{103}$$

The wavenumber with the largest growth rate is given by

$$\frac{k_*(T)}{k_0} = \left[\left(\frac{T_c}{T} \right)^{1/2} - 1 \right]^{1/2}, \tag{104}$$

and the largest growth rate by

$$\frac{2\sigma_*}{\xi} = -1 + \sqrt{1 + \frac{4 S_d G \rho}{\xi^2} \left[1 - \left(\frac{T}{T_c} \right)^{1/2} \right]^2}. \tag{105}$$

The maximum wavenumber $k_{max}(T)$ and the most unstable wavenumber $k_*(T)$ are plotted as a function of the temperature in Figure 9. In Figure 10, we represent the growth rate $\sigma(k)$ as a function of the wavenumber. Finally, in Figure 11, we plot the largest growth rate $\sigma_*(T)$ as a function of the temperature. The maximum value of the largest growth rate $\sigma_*(T)$ is obtained for $T = 0$ and is given by

$$\frac{2(\sigma_*)_{max}}{\xi} = -1 + \sqrt{1 + \frac{4 S_d G \rho}{\xi^2}}. \tag{106}$$

For $k_0 = 0$ (Newtonian interaction), then $T_c = +\infty$ and the growth rate of the perturbation can be expressed as

$$\frac{2\sigma}{\xi} = -1 + \sqrt{1 - \frac{4 k^2}{\xi^2} \left(T - \frac{S_d G \rho}{k^2} \right)}. \tag{107}$$

The condition of instability is

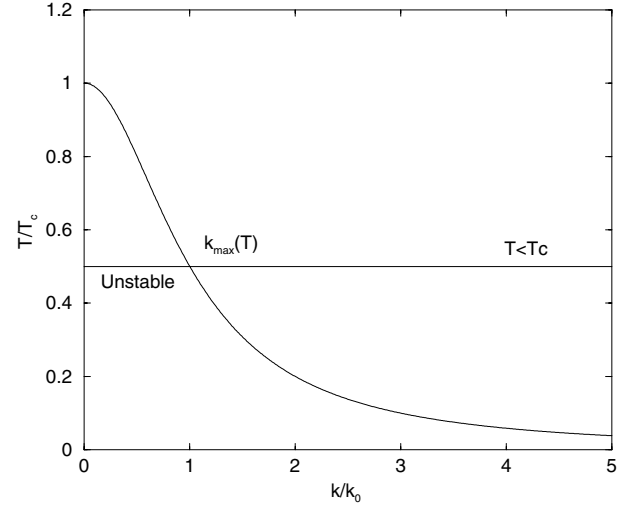$$k \leq k_{max} = \left(\frac{S_d G \rho}{T} \right)^{1/2}, \tag{108}$$

Fig. 8. Graphical construction determining the range of unstable wavenumbers.
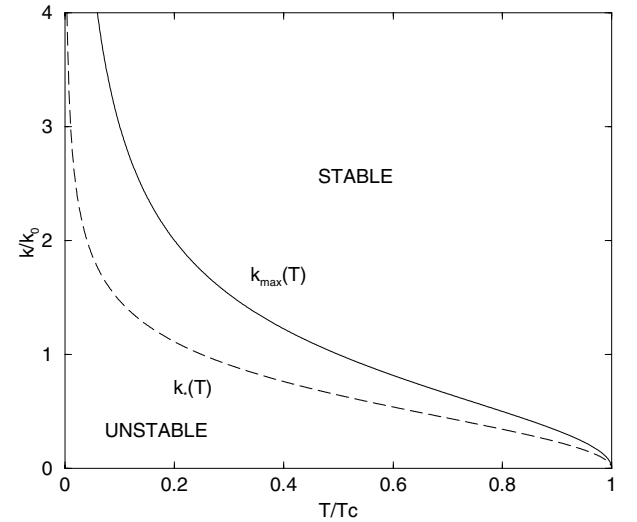

Fig. 9. Maximum wavenumber $k_{max}(T)$ and most unstable wavenumber $k_*(T)$ as a function of the temperature T. The line $k_{max}(T)$ determines the separation between stable and unstable states.

where k_{max} is the equivalent of the Jeans wavenumber. The maximum growth rate is obtained for $k_* = 0$ and its value is given by

$$\frac{2\sigma_*}{\xi} = -1 + \sqrt{1 + \frac{4 S_d G \rho}{\xi^2}}, \tag{109}$$

independently of the temperature. The growth rate $\sigma(k)$ is represented as a function of the wavenumber in Figure 12.

4 Conclusion

In this paper, we have studied the linear dynamical stability of an infinite and homogeneous distribution of biological cells whose density distribution evolves under the
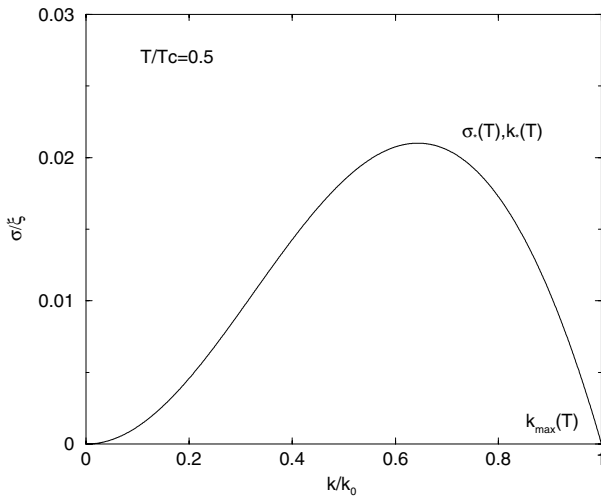
Fig. 10. Growth rate of the perturbation as a function of the wavenumber. We have taken $4S_dG\rho/\xi^2 = 1$ and $T/T_c = 0.5$.
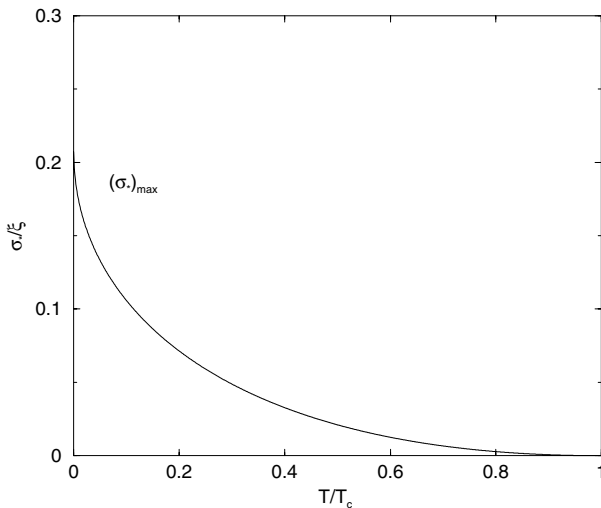

Fig. 11. Dependence of the largest growth rate $\sigma_*(T)$ with the temperature. We have taken $4S_dG\rho/\xi^2 = 1$.

Fig. 12. Growth rate $\sigma(k)$ as a function of the wavenumber when $k_0 = 0$. We have taken $4S_dG\rho/\xi^2 = 1$. In terms of the variable $k/k_{max}(T)$, the curve is independent on the temperature.

process of chemotaxis. We have modeled their evolution by hydrodynamical equations including a friction force [8,9]. This inertial model takes into account the fact that the cells do not respond immediately to the chemotactic drift but that there is a relaxation time ξ^{-1} for their velocity to get aligned with the chemotactic gradient. The usual Keller-Segel model [2] is recovered in the strong friction limit $\xi \to +\infty$ (or for large times $t \gg \xi^{-1}$). Alternatively, for $\xi = 0$, we recover the inertial model of [3]. We have shown that these equations were similar to those describing self-gravitating Brownian particles and that the dynamical stability of biological populations was related to the Jeans problem in astrophysics. These results extend the analogies between biology and astrophysics investigated in [9].

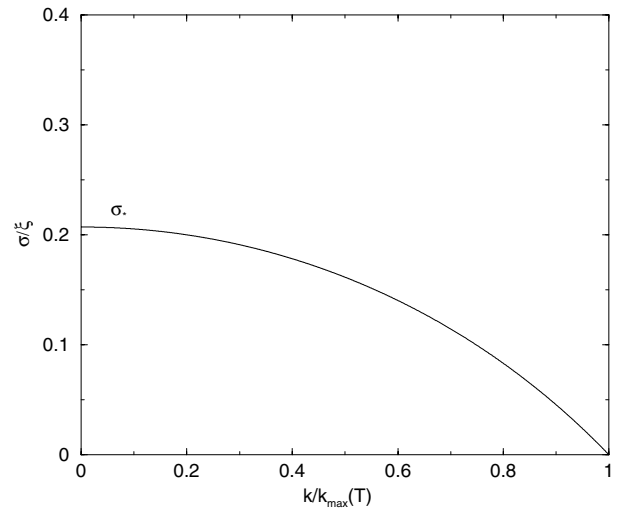The mathematical model (6)-(8) considered in this paper can have applications in biology. Depending on the value of the parameters, it can describe different sorts of systems. The Keller-Segel model (1)-(2) obtained in the overdamped limit $\xi \to \infty$ in which inertial terms can be neglected is appropriate to describe experiments on bacteria like *Escherichia Coli* and slime mold amoebae like *Dictyostelium discoideum* [2]. These systems exhibit pointwise concentrations as a result of chemotactic collapse. On the other hand, the hydrodynamic model (3)-(5) was shown to generate a vascular network starting from randomly seeded endothelial cells [3,4]. This can account for experiments of in vitro formation of blood vessels where cells randomly spread on a gel matrix autonomously organize to form a connected network that can be interpreted as the initiation of angiogenesis. This is also similar to the formation of capillary blood vessels in living beings during embriogenesis [16]. The authors of [3] evidence a percolative transition as a function of the concentration of cells. Above a critical density, the system forms a continuous multi-cellular network which can be described by a collection of nodes connected by chords. For even higher concentrations a "swiss cheese" pattern is observed. Such structures can be obtained only if inertial terms are accounted for. Another hydrodynamic model of bacterial colonies taking into account interial terms has been proposed by Lega and Passot [17] to describe the evolution of bacterial colonies growing on soft agar plates. This model consists in advection-reaction-diffusion equations for the concentrations of nutrients, water, and bacteria, coupled to a single hydrodynamic equation for the velocity field of the bacteria-water mixture. This model is able to reproduce the usual colony shapes together with nontrivial dynamics inside the colony such as vortices and jets recently observed in wet colonies of *Bacillus subtilis* [18]. This can be linked to a process of inverse cascade of energy as in two-dimensional hydrodynamic turbulence. Lega and Passot [17] show that the large-scale Reynolds numbers can be relatively high so that inertial effects have

to be taken into account to adequately model the experiments of [18]. It is shown also that viscosity is important in this model. Although the hydrodynamic equations of [17] are different from equations (6–8), their model displays a mechanism for collective motion towards fresh nutrients which is similar to classical chemotaxis. In particular, a chemotacticlike behaviour and a connection to the Keller-Segel model (1)-(2) is obtained for short times.

In this paper, we have considered solutions of equations (6–8) near an infinite and homogeneous distribution and we have investigated the time dependence of these solutions in the linear regime[1]. When the criterion (18) is fulfilled, the appearance of a spontaneous perturbation can lead to an instability. The perturbation grows until the system can no longer be described by equilibrium or near-equilibrium equations. In that case, we must account for the full nonlinearities encapsulated in equations (6–8). Of course, the nonlinear regime of instability is the most relevant for biological applications. This nonlinear regime has been investigated in detail for a reduced version of the Keller-Segel model [13]:

$$\frac{\partial \rho}{\partial t} = D\Delta\rho - \chi \nabla \cdot (\rho \nabla c), \qquad (110)$$

$$\Delta c = -\lambda \rho. \qquad (111)$$

In that case, the concentration of the chemical is related to the concentration of the bacteria by a Poisson equation. These equations are isomorphic to the Smoluchowski-Poisson system

$$\frac{\partial \rho}{\partial t} = \nabla \cdot \left[\frac{1}{\xi} \left(T\nabla\rho + \rho\nabla\Phi \right) \right], \qquad (112)$$

$$\Delta\Phi = S_d G\rho, \qquad (113)$$

describing self-gravitating Brownian particles [11]. In dimension $d \geq 2$, they exhibit blow-up solutions leading ultimately to the formation of Dirac peaks. This corresponds to a chemotactic collapse in biology or to an isothermal collapse (in the canonical ensemble) in gravity. There is a vast literature on the theoretical study of these equations both in applied mathematics (see the review by Horstmann [19]) and in physics [10,11,20–22]. Generalized chemotactic models and generalized gravitational models have also been studied, like in [23] to account for anomalous diffusion or like in [10] to account for inertial effects. On the other hand, bifurcations between "stripes" and "spots" have been found when the degradation of the secreted chemical is taken into account so that the equilibrium structures of the bacterial colonies are similar to "domain walls" in phase ordering kinetics [24]. The linear

instability regime that we have considered in this paper initiates the nonlinear regime where interesting and nontrivial structures form, accounting for the morphogenesis of bacterial populations. In the linear instability analysis, the general form of perturbation is a superposition of sinusoidal waves. Each single wave corresponds to a "streak" with relatively high density. However, other patterns like regularly spaced "clouds" can be obtained by a proper superposition of "streaks" (see Appendix A of [2]). These "clouds" will be presumably selected by nonlinear effects and each of them can initiate a local collapse leading to pointwise blow-up [11,19,20]. Indeed, these clouds have the radial symmetry that is assumed at the start in most studies of chemotactic collapse. This will lead to a set of N singular structures. These compact structures interact with each other and lead to a coarsening process where the number of clusters decays in time as they collapse to each other. This process may share some analogies with the aggregation of vortices in two-dimensional decaying turbulence [25]. Therefore, the connection between the linear regime investigated in this paper and the nonlinear regime investigated in [11,19,20] is relatively clear.

References

1. J.D. Murray, *Mathematical Biology* (Springer, Berlin, 1991)
2. E. Keller, L.A. Segel, J. theor. Biol. **26**, 399 (1970)
3. A. Gamba et al., Phys. Rev. Lett. **90**, 118101 (2003)
4. F. Filbet, P. Laurençot, B. Perthame, J. Math. Biol. **50**, 189 (2005)
5. J. Peebles, *Large-Scale Structure of the Universe* (Princeton University Press, 1980)
6. M. Vergassola, B. Dubrulle, U. Frisch, A. Noullez, Astron. Astrophys. **289**, 325 (1994)
7. P.H. Chavanis, J. Sommeria, R. Robert, Astrophys. J. **471**, 385 (1996)
8. P.H. Chavanis, Phys. Rev. E **68**, 036108 (2003)
9. P.H. Chavanis, M. Ribot, C. Rosier, C. Sire, Banach Center Publ. **66**, 103 (2004)
10. P.H. Chavanis, C. Sire, Phys. Rev. E **73**, 066103 (2006); Phys. Rev. E **73**, 066104 (2006)
11. P.H. Chavanis, C. Rosier, C. Sire, Phys. Rev. E **66**, 036105 (2002)
12. J.H. Jeans, *Astronomy and Cosmogony* (Cambridge University Press, 1929)
13. W. Jäger, S. Luckhaus, Trans. Am. Math. Soc. **329**, 819 (1992)
14. J.P. Cox, *Theory of Stellar Pulsation* (Princeton Series in Astrophysics, 1980)
15. J. Binney, S. Tremaine, *Galactic Dynamics* (Princeton Series in Astrophysics, 1987)
16. P. Carmeliet, Nature Medicine **6**, 389 (2000)
17. J. Lega, T. Passot, Phys. Rev. E **67**, 031906 (2003)
18. N.H. Mendelson et al., J. Bacteriol. **181**, 600 (1999)
19. D. Horstmann, Jahresberichte der DMV **106**, 51 (2004)
20. C. Sire, P.H. Chavanis, Phys. Rev. E **66**, 046133 (2002)
21. C. Sire, P.H. Chavanis, Phys. Rev. E **69**, 066109 (2004)
22. P.H. Chavanis, C. Sire, Phys. Rev. E **70**, 026115 (2004)
23. P.H. Chavanis, C. Sire, Phys. Rev. E **69**, 016116 (2004)
24. P.H. Chavanis, e-print [arXiv: physics/0607020]
25. C. Sire, P.H. Chavanis Phys. Rev. E **61**, 6644 (2000)

---

[1] The linear dynamical stability of *inhomogeneous* distributions of bacteria has also been studied in [11,20] for over-damped models and in [10] for inertial models, when the equation for the concentration of the chemical takes the form of a Poisson equation (111) like in gravity. In these studies, the distribution of particles is self-confined [10] or confined in a finite domain (box) [11,20]. In biology, the box can represent a droplet or the container itself.